Department of Physics and Astronomy
University of Heidelberg

Bachelor Thesis in Physics
submitted by

Alexandra Alice Beikert

born in Heidelberg (Germany)

2021

Controlled Frequency Generation for Grey Molasses Cooling

This Bachelor Thesis has been carried out by Alexandra Alice Beikert at the
Kirchhoff-Institute for Physics in Heidelberg
under the supervision of
Prof. Markus Oberthaler

Abstract

Controlled Frequency Generation for Grey Molasses Cooling

This thesis presents the design and implementation of two approaches to generate stable frequencies, the sum of which is kept constant. The first approach locks the sum of two frequencies to a reference signal, using a feedback system called a phase-locked loop. The second technique produces the desired frequency by directly generating the difference of a stable reference frequency and an input frequency. This second approach is implemented to generate RF frequencies for grey molasses cooling on a Potassium-39 cold atom experiment. The presented implementation and optimisation of the new frequency-generated system decreases the temperature by 30%, while the atom number increases by 20%. Additionally, the system has demonstrated long-term stability.

Erzeugung aufeinander abgestimmter Frequenzen für das Kühlen mit einer grauen Molasse

Diese Arbeit präsentiert den Entwurf und die Implementierung von zwei Methoden zur Erzeugung stabiler Frequenzen, deren Summe konstant gehalten wird. Die erste Methode regelt die Summe zweier Frequenzen auf ein Referenzsignal, wobei ein Rückkopplungssystem verwendet wird, das als Phasenregelschleife bezeichnet wird. Die zweite Methode erzeugt die gewünschte Frequenz durch Bilden der Differenz einer stabilen Referenzfrequenz mit einer Eingangsfrequenz. Dieser zweite Ansatz wird implementiert, um RF-Frequenzen für die Kühlung von Kalium-39 Atomen mit einer grauen Melasse zu erzeugen. Nach der Implementierung und Optimierung der neuen frequenzerzeugenden Systems wurde die Temperatur der grauen Melasse um 30% gesenkt, während die Atomzahl um 20% erhöht wurde. Darüber hinaus hat sich das System als langzeitstabil erwiesen.

Contents

1 Introduction

To study effects like Bose-Einstein condensation or to build atomic clocks, atoms at temperatures near absolute zero are crucial. One reaches these temperatures by using laser cooling, the basis of which was developed in the 1980s by William Philips, Steven Chu and Claude Cohen-Tannoudj [12, 6, 2, 4]. Their approach allows cooling down to temperatures of a few microkelvins, for which they were awarded the Nobel Prize in Physics in 1997.

One possible laser cooling technique are optical molasses, consisting of six counterpropagating red-detuned laser beams. With optical molasses one can reach temperatures well below the Doppler limit, which can be explained by taking the hyperfine structure of an atom into account. This effect is called Sisyphus cooling [9]. The final temperature depends on the atoms used: with potassium-39 atoms (^{39}K), temperatures up to 25μK were reached [8].

An improvement to optical molasses are grey molasses, which combine Sisyphus cooling with velocity selective coherent population trapping. The main difference to optical molasses is that they use two light fields with different frequencies which drive different transitions in the atom. With grey molasses, temperatures up to 6μK are possible [13].

An important requirement for grey molasses cooling is that the two light fields fulfil the Raman condition, i.e., the frequency difference between the two light fields must be stable. Furthermore, the two frequencies need to be tuneable.

In the BECK experiment in Heidelberg, ^{39}K atoms are cooled down to a few nanokelvins, resulting in a two dimensional Bose-Einstein condensate. In this experimental setup the control of the laser frequencies for the grey molasses was implemented using two independent computer channels. This leads to the disadvantage that one can only indirectly control the frequency difference and thus the Raman condition.

In this Bachelor thesis, I discuss two different solutions to stabilise the frequency difference and to optimise cooling. One is based on a frequency mixer and a phase-locked loop; the other one is simpler and only based on a frequency mixer.

This thesis starts with a short introduction of the theory of grey molasses cooling. Since frequency mixers play an important role in both setups, I examine them closely in section 3 and test them in section 4. In section 5 and section 6, I introduce two setups to generate the frequencies necessary for the implementation of the molasses. For one of the setups, I show the implementation in the BECK experiment and the cooling performance. Finally, I conclude with summarising my results.

2 Grey Molasses Cooling

In this section, I introduce the principle of grey molasses cooling. First, I explain laser cooling in optical molasses, based on a two-level system. Then, I explain a three-level system, the basis for grey molasses cooling. I outline the principle of grey molasses cooling and how one determines the final temperature. I conclude with the generation of the laser frequencies and how this can be used to stabilise the frequency difference of the laser fields.

2.1 Laser Cooling using Optical Molasses

A laser cooling method is optical molasses, consisting of six counterpropagating red-detuned laser beams. The atoms are in the middle of the beams and absorb photons of the lasers. Since momentum is conserved the velocity of the atoms changes. Each atom emits the absorbed photon afterwards, but in a random direction, which averages out. Due to the Doppler effect, the frequency to which the atoms react changes. The detuning in frequency is necessary so that photons excite only atoms moving towards the respective laser beam. This accelerates the atoms in the direction of the laser beam, decelerating them to the Doppler limit in this simplified depiction.

As Boltzmann's law states that the temperature of an atomic cloud is proportional to the mean velocity, this cools the atoms.

In this depiction, with optical molasses, one can reach temperatures up to the Doppler limit

$$T_D = \frac{\hbar\gamma}{2k_B}, \tag{1}$$

with γ the natural linewidth of the used energy level. Temperatures below the Doppler limit can be explained with the hyperfine structure of an atom, which is then called Sisyphus cooling [9].

2.2 Three-Level System

Optical molasses base on a two-level system. Lower temperatures can be reached with grey molasses, which base on a three-level system. The following section explains the three-level-system in a simplified approach.

Two ground states $|1\rangle$,$|2\rangle$ with equal energy, but different Rabi frequencies Ω_1 and Ω_2 interact with an excited state $|3\rangle$ in a blue detuned light field with frequency ω.

The Hamiltonian in the rotating frame approximation is then given by the sum of the Hamiltonian H_0 without light interaction and the coupling Hamiltonian V. In the following, I identify state $|i\rangle$ with the basis vector $\mathbf{e}_i$.

$$H = H_0 + V = \frac{\hbar}{2}\begin{pmatrix} 0 & 0 & 0 \\ 0 & 0 & 0 \\ 0 & 0 & -2\delta \end{pmatrix} + \frac{\hbar}{2}\begin{pmatrix} 0 & 0 & \Omega_1 \\ 0 & 0 & \Omega_2 \\ \Omega_1 & \Omega_2 & 0 \end{pmatrix} \tag{2}$$

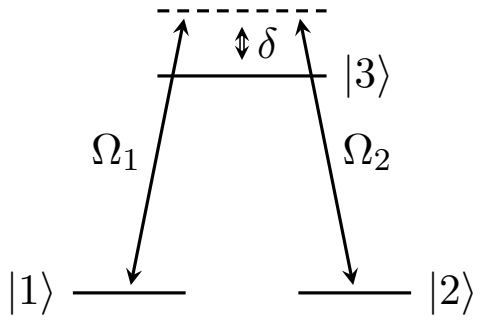

Figure 1: Three level system: A laser field drives blue-detuned transistions between ground states $|1\rangle$ and $|2\rangle$ with Rabi frequency Ω_1 and Ω_2 and the excited state $|3\rangle$. δ defines the detuning.

Diagonalising the Hamiltonian leads to new eigenvectors and eigenstates:

$$\begin{aligned}
\lambda_D &= 0 \\
\lambda_{B_1} &= -\delta - \sqrt{\Omega_1^2 + \Omega_2^2 + \delta^2} \\
\lambda_{B_2} &= -\delta + \sqrt{\Omega_1^2 + \Omega_2^2 + \delta^2} \\
|\psi_D\rangle &= -\frac{\Omega_1}{\Omega_2}|1\rangle + |2\rangle \\
|\psi_{B_1}\rangle &= \frac{\Omega_1}{\lambda_{B_1}}|1\rangle + \frac{\Omega_2}{\lambda_{B_1}}|2\rangle + |3\rangle \\
|\psi_{B_2}\rangle &= \frac{\Omega_1}{\lambda_{B_2}}|1\rangle + \frac{\Omega_2}{\lambda_{B_2}}|2\rangle + |3\rangle
\end{aligned}$$

One can easily see that $|\psi_D\rangle$ does not couple with $|3\rangle$ anymore: It is a dark state, meaning that no transitions to $|3\rangle$ and thus to the other eigenstates can be driven once reaching this state.

$|\psi_{B_1}\rangle$ and $|\psi_{B_2}\rangle$ are bright states: They can decay in every other state, including the dark state.

In our grey molasses setup, the energy difference between the two ground states is not zero. This leads to a perturbation term on the diagonal of H_0 which complicates the system.

2.3 Grey Molasses

In this subsection, I explain the implementation of the three-level system for grey molasses. I focus on grey molasses for ^{39}K potassium atoms, using the D1 transition. They principle stays the same for other atoms.

The ground states $^2S_{1/2}$ are given by the hyperfine splitting, as depicted in Figure 2. Two ground states lead to a three-level system. The used excited state is the $^2P_{1/2}$ $F = 2$ state.

The energy difference between the ground states is nonzero and is given by 461.7 MHz. For that reason, two light fields are needed: One for the repumping transition from the $F = 1$ ground state and one for the cooling transition from the $F = 2$ ground state.

The experimental setup consists of six counter-propagating laser beams, as in the optical molasses. In the grey molasses, in each laser beam, both light field frequencies overlap. The laser beams have an opposing polarisation which leads to a polarisation gradient. The Rabi

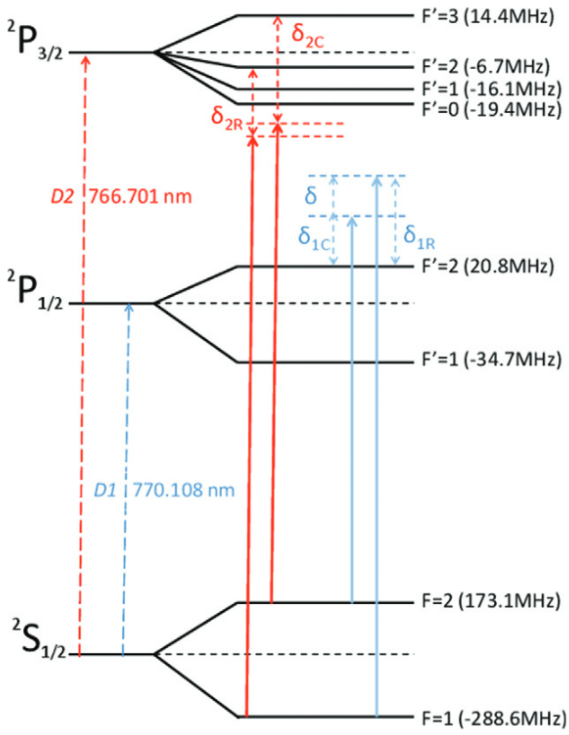

Figure 2: Optical transitions of the D1 and D2 lines of ^{39}K with their laser detunings δ_1 and δ_2. The subscripts R and C refer to the repumping and cooling transitions. The transition used for grey molasses cooling is the D1 transition with ground states $^2S_{1/2}$ with $F = 1, 2$ and excited state $^2P_{1/2}$ $F = 2$, shown by the blue lines. Taken from [13]

frequencies are getting spatially dependent and thus the energy eigenvalues for the two bright states oscillate.

Since the atoms have a velocity, a kinetic term appears in the Hamiltonian, which leads to motional coupling: Transitions from the dark state to the potential minimum of the bright states are possible for moving atoms. By climbing the potential hill of the polarization gradient, the atom loses speed and can decay back into the dark state. Averaging these processes, the atom loses energy as the probability to couple to the bright state is maximal at the minimum of the gradient potential. Figure 3 shows this behaviour.

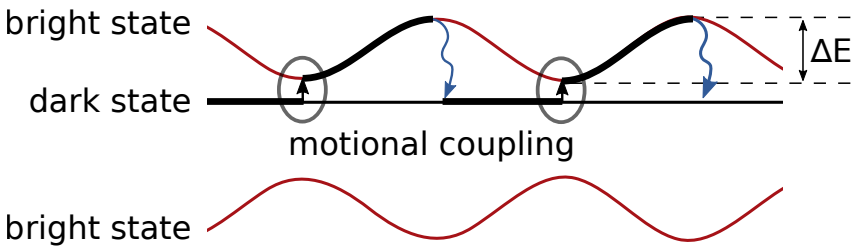

Figure 3: A schematic picture of grey molasses cooling. Due to the spatially dependent Rabi frequencies, the energy eigenvalues for the two bright states, shown in red, oscillate. Motional coupling allows transitions from the dark state to a minimum of the bright state. By climbing the potential hill, the atom loses speed and can decay back into the dark state. Averaging these processes leads to an energy loss and to a lower temperature.

When the atom is slow enough, it stays in the dark state: Maximum cooling is reached. The cooling force acts inversely proportional to the detuning: The lower the detuning, the higher the cooling force. To get a maximal cooling force, one sets the cooler frequency close to the resonance frequency and waits until the temperature is cold enough. Waiting too long leads to atoms leaving the molasses.

In reality, we do not have a completely dark state since there are many levels nearby, which limits the cooling. It is called a grey state. The grey state leads to a reheating force Γ which is inversely proportional to δ^2. To minimise the reheating, one increases the detuning after a hold time, called ramping. Since the atoms are already cold, cooling isn't affected by this.

To sum up, different parameters affect the minimal cooling temperature: The frequency difference between the two light fields needs to be stable and fulfil the Raman condition. The hold time has to be sufficiently long to cool, while still keeping the atoms in the molasses. Also, the detuning must be adjustable during ramping.

2.4 Determination of the Final Temperature

A key indicator for the performance of the grey molasses is the final temperature reached. Grey molasses cooling slows the atoms, but the atomic cloud still expands since grey molasses do not trap the atoms. The final temperature is proportional to the expanding velocity of the atomic cloud, which is determined by measuring its width σ_x after a time-of-flight expansion. The squared width of the velocity distribution is then given by

$$\sigma_x^2 = \sigma_{x_0}^2 + \sigma_v^2 t^2, \tag{3}$$

with σ_v the width of the velocity distribution. One can determine σ_v by a linear fit. The temperature is then proportional to σ_v^2,

$$T = \frac{\sigma_v^2 m}{k_B}, \tag{4}$$

with the mass of the atom m and the Boltzmann factor as proportionality constant. Figure 4 shows the linearity in the old molasses setting with a slope of $\sigma_v^2 = 1.96 \cdot 10^7$. Here, σ_x is given in pixels. Calibration needs a factor $[9.47 \cdot 10^{-6}]^2$, which leads, together with Equation 4 and $m = 39u$ for ^{39}K to a temperature of 11μK. Since the measured data approximates a linear fit, it is sufficient to measure the distribution width after one time of flight to get a precise guess of the final temperature.

2.5 Frequency Modulation of Laser Light

As explained, grey molasses cooling needs two laser fields with a fixed frequency difference. Figure 2 shows that both laser field frequencies vary about $\pm$230MHz from the D1 transition frequency. In the experimental setup, two Acousto-Optic Modulators (AOM) [10] shift the laser frequencies according to the D1 transition, which is locked close to the crossover. One is generating the repumping frequency by reducing the D1 frequency by f_1, the other one is generating the cooling frequency by increasing the D1 frequency by f_2. The amount of

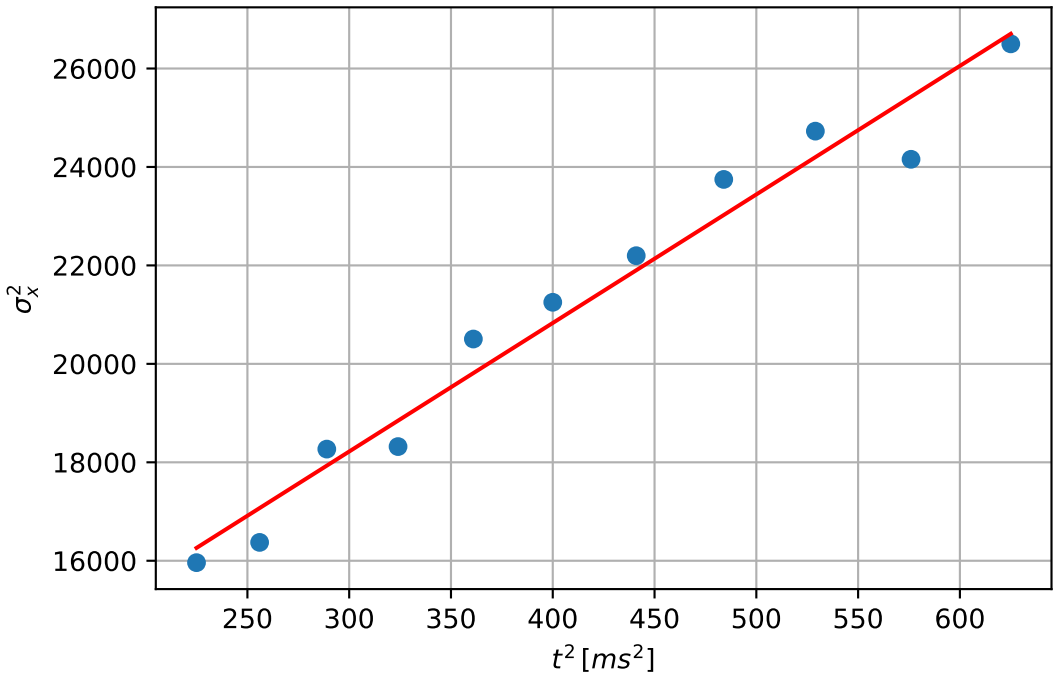

Figure 4: Time of flight in the old grey molasses setting. Depicted is the distribution width σ_x^2 after different time of flights in ms^2. The slope of the linear fit, highlighted in red, gives with $1.96 \cdot 10^7$ the velocity distribution width σ_v^2, which is proportional to the final temperature, here 11μK.

increase/reduction depends on the detuning δ and the energy difference of the states. The sum of the increasing and reducing frequency in MHz defines the energy difference and thus the Raman condition: $f_1 + f_2 = 461.7$MHz. In the following, I work with the frequencies f_1 and f_2 going to the AOMs and I stabilise the sum of those frequencies. Since double pass AOMs are used, the sum reduces to 230.85MHz.

3 Frequency Mixers

For our application of stabilising the Raman condition, we need the sum of two frequencies. This can be achieved by frequency mixing. In this section, I motivate the principle of mixing and why mixers are needed. Afterwards, I explain the working principle of a ring modulator mixer.

3.1 Frequency Mixing

It is impossible to sum or subtract frequencies by simply adding different signals in the same cable or other linear elements. The superposition of two oscillating voltages will simply lead to the sum of the two signals. To create a signal that oscillates with the sum of their frequencies, one needs a non-linear element. A non-linear element can create higher orders of the sum. Starting with two signals, each signal is given by

$$A(t) = A\cos\omega t, \tag{5}$$

and one can write the sum of these two signals in the following way. A non-linearity is given by squaring the sum

$$\begin{aligned}(A\cos\omega_1 t + B\cos\omega_2 t)^2 = \frac{1}{2}A^2 + \frac{1}{2}B^2 + \frac{1}{2}A^2\cos 2\omega_1 t + \frac{1}{2}B^2\cos 2\omega_2 t \\ + AB\cos((\omega_1-\omega_2)t) + AB\cos((\omega_1+\omega_2)t).\end{aligned} \tag{6}$$

By squaring the sum of two signals, one gets signals with the sum and the difference of the original frequencies, as well as terms with twice the frequency. For that reason, a typical frequency mixer needs a non-linear element.

In electronics, one of the simplest non-linear elements are diodes: Diodes have an exponential current–voltage characteristic, given by the Shockley diode equation

$$I = I_S(\exp\left\{\frac{V_D}{nV_T}\right\} - 1). \tag{7}$$

I is the diode current, I_S the scale current, V_D is the voltage across the diode, V_T is the thermal voltage, given by the Boltzmann constant times temperature divided by electron charge. n is the quality factor. In the ideal case, n is set to 1. The non-linearity becomes clear by writing the exponential in its series representation

$$\exp\{x\} = \sum_{n=0}^{\infty}\frac{x^n}{n!} \tag{8}$$

which contains not only the quadratic but also higher order terms. In a second-order approximation, one can assume the exponential as quadratic term. This simple example shows how a non-linear operation can mix the frequency of two signals.

Based on non-linear elements several different mixer designs are possible. Here, I will focus on a ring modulator design.

3.2 Ring Modulators

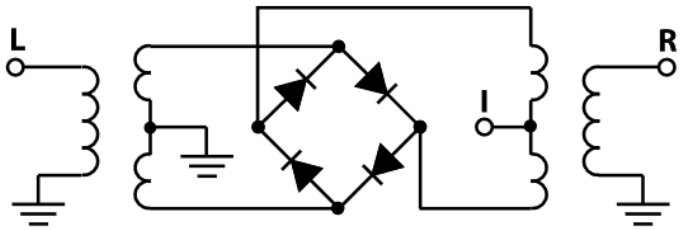

Figure 5: Circuit diagram of a ring modulator. L and R are inputs, representing the Local Oscillator (LO) signal and the RF signal. I is the output, i.e., the mixed signal. The LO signal, transmitted by induction, switches diodes on and off. Depending on the switched-on diodes, either the RF signal or the inverted RF signal is grounded. Taken from [11]

A ring modulator is a mixer that produces only the sum and the difference in first order approximation of two incoming signals and suppresses the original frequencies. Figure 5 shows its circuit diagram. The inputs are left and right. The circuit is completely symmetric, but for unambiguity, one names the left input the local oscillator (LO) input and the right input the radio frequency (RF) input. The input signals are transferred to the main circuit by induction. The main circuit consists of four diodes, arranged in a ring. It is a similar structure to a rectifier, but with two diodes flipped. Ground is between the two LO coils. The Output (I or IF) is between the two RF coils.

Ring modulators operate by switching: If the LO signal is significantly higher in amplitude than the RF signal, the LO signal switches diodes on and off. Figure 6 depicts this. If the LO Power is positive, diodes D_2 and D_3 are blocked and diodes D_1 and D_4 conduct. The RF signal appears at the output. If the LO Power is negative, diodes D_2 and D_3 conduct and diodes D_1 and D_4 are blocked. The negative RF signal appears at the output.

The RF signal passes to the IF output, but the sign depends on the LO signal. Simplified, the output is then given by a multiplication of the two input signals

$$IF = A_{RF} \cos \omega_{RF} \cos \omega_{LO} = \frac{A_{RF}}{2} [\cos(\omega_{RF} + \omega_{LO}) + \cos(\omega_{RF} - \omega_{LO})]. \tag{9}$$

Figure 7 illustrates this. The only remaining frequencies are the sum and the difference frequency. The only relevant amplitude for the IF output is the amplitude of the RF signal.

Up to this point, I only considered the first order approximation. However, in the ring modulator output, besides the sum and difference, various intermodulation frequencies occur. These can be explained by again looking at the LO signal: Since the ring modulator operates by switching the diodes, only its sign is relevant. This is equivalent to approximating the sine wave with a square wave. One can write the sign of the linear oscillator signal as the fourier transform of the rectangular signal,

$$\text{rect} = \sin \omega t + \frac{1}{3} \sin 3\omega t + \frac{1}{5} \sin 5\omega t + \dots \tag{10}$$

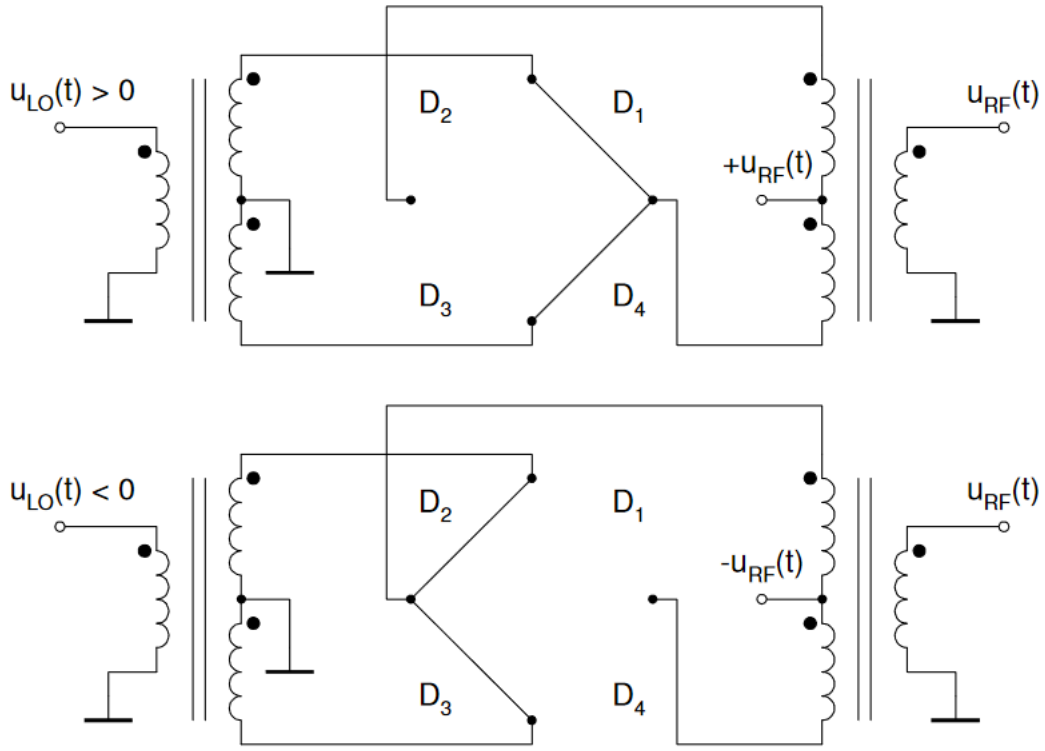

Figure 6: Diode switching behaviour of a ring modulator. The local oscillator signal is higher in amplitude and switches the diodes on and off. Diodes 1 and 4 conduct when the LO voltage is positive, and the RF signal appears at the output. Diodes 2 and 3 conduct when the LO voltage is negative, and the inverted RF signal appears at the output. This leads to a product of the LO and RF signal at the output. Taken from [7]

and the output is the product of this fourier series with the RF signal. That complicates Equation 9 to products of different frequencies. Intermodulation terms occur.

Belevitch [3] determined the amplitudes V_{mn} of the components of frequency $m\omega_{LO} \pm n\omega_{RF}$. He stated that the amplitudes are

$$\frac{V_{mn}}{V_c} = \frac{k^n \Gamma(\frac{m+n-1}{2})}{\pi \Gamma(n+1)\Gamma(\frac{m-n+3}{2})} F(\frac{m+n-1}{2}, \frac{m-n+1}{2}, n+1; k^2), \tag{11}$$

where F is the hypergeometric function and k the ratio V_s/V_c. V_s is the amplitude of the signal voltage (RF) and V_c the amplitude of the carrier voltage (LO). Belevitch deduced from this formula that only products corresponding to odd values of m and n exist due to the balance of the modulator. For small signal voltages (RF « LO) and thus small k, the dominant products are $m\omega_{LO} \pm \omega_{RF}$.

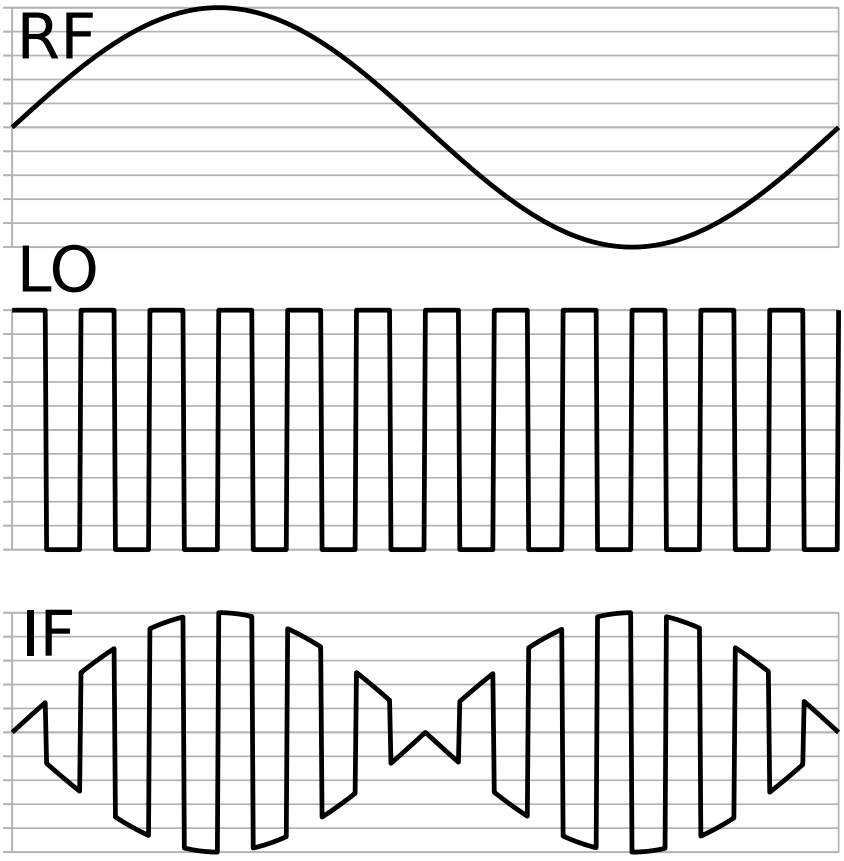

Figure 7: Principle of ring modulation. The LO signal (middle picture) is switching the diodes on and off and can thus be assumed as rectangular. It affects the sign of the RF signal (top picture). The output signal (bottom picture) is the product of the input signals. Adapted from [16]

4 Measuring Mixing Performance

The previous section explains the theoretical behaviour of a ring modulator in detail. In this section, I test a mixer in the frequency range needed to stabilise the grey molasses, i.e., radio frequencies of around 100MHz. I show that the output of a mixer is indeed the sum frequency and difference frequency and that the predicted intermodulation terms occur. In addition, I examine the effect of using the same amplitudes for both input frequencies on the mixer, representing an incorrect operation mode.

4.1 Voltage Controlled Oscillator

To generate the frequencies for testing the mixer I employ a Voltage Controlled Oscillator (VCO). The VCO generates a sine wave with a frequency proportional to its tuning voltage. The characteristic depends on the VCO used. Here, I use a POS-150. Figure 8 shows the linear relation between the tuning voltage on the x-axis and the output frequency on the y-axis.

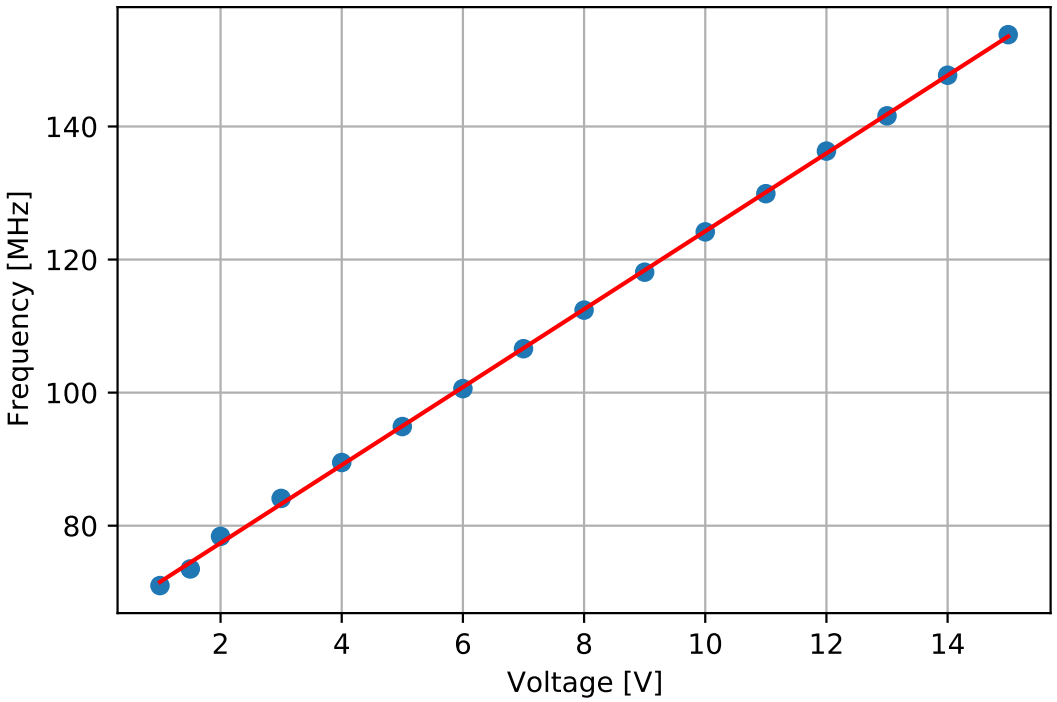

Figure 8: Characteristic of the Voltage Controlled Oscillator (VCO) POS-150. The VCO generates a frequency proportional to a tuning voltage. Possible tuning voltages are between 1V and 15V, corresponding to frequencies between 70MHz to 150MHz. The blue dots are the measured characteristic, the red line is a linear fit. The linearity for the POS-150 is given by $f(U) = 65.68\text{MHz} + 5.86\frac{\text{MHz}}{\text{V}} \cdot \text{U}$

Possible values are between 1V and 15V. The respective frequency is determined with a spectrum analyser and between 70MHz to 150MHz. The slope in Figure 8 gives the VCO

characteristic of the POS-150

$$f(U) = 65.68\text{MHz} + 5.86\frac{\text{MHz}}{\text{V}} \cdot \text{U}, \tag{12}$$

where f is the generated frequency when tuning the VCO with a voltage U.

Figure 9 shows a typical output signal of the VCO for a tuning voltage of 6V on a spectrum analyser. The main peak is at 99MHz. The signal is measured behind a directional coupler which is a power divider and attenuates the signal from 9dBm to −2dBm.

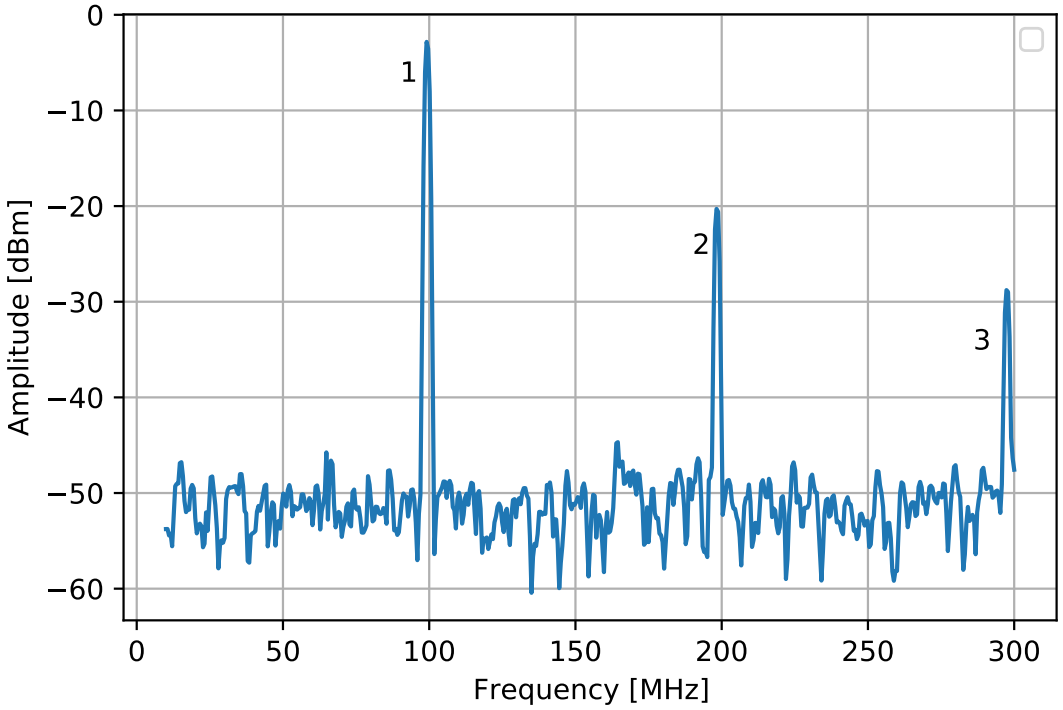

Figure 9: The output of a VCO behind a directional coupler on a spectrum analyser. The tuning voltage is 6V. The directional coupler is a power divider and attenuates the signal about 10dB. The figure shows the output frequency at 99MHz (peak 1), as well as the less dominant higher harmonics at $2 \cdot 99$MHz (peak 2) and $3 \cdot 99$MHz (peak 3). The generated frequency bandwidth is narrower than in the figure, which is limited in resolution.

The figure also shows the higher harmonics at the double and the triple frequency. The generated frequency bandwidth is narrower than in the figure, which is limited in resolution. The noise of the signal is small.

4.2 Mixing Behaviour

In section 3 I discuss the usage of a mixer. Recall that a mixer has two inputs and one output. One input is the local oscillator (LO). The LO needs to be high in amplitude to switch the diodes. The other input is the RF signal. Here, the power needs to be around 10dB smaller than the power of the LO. In the following experiments, the LO signal is held constant at

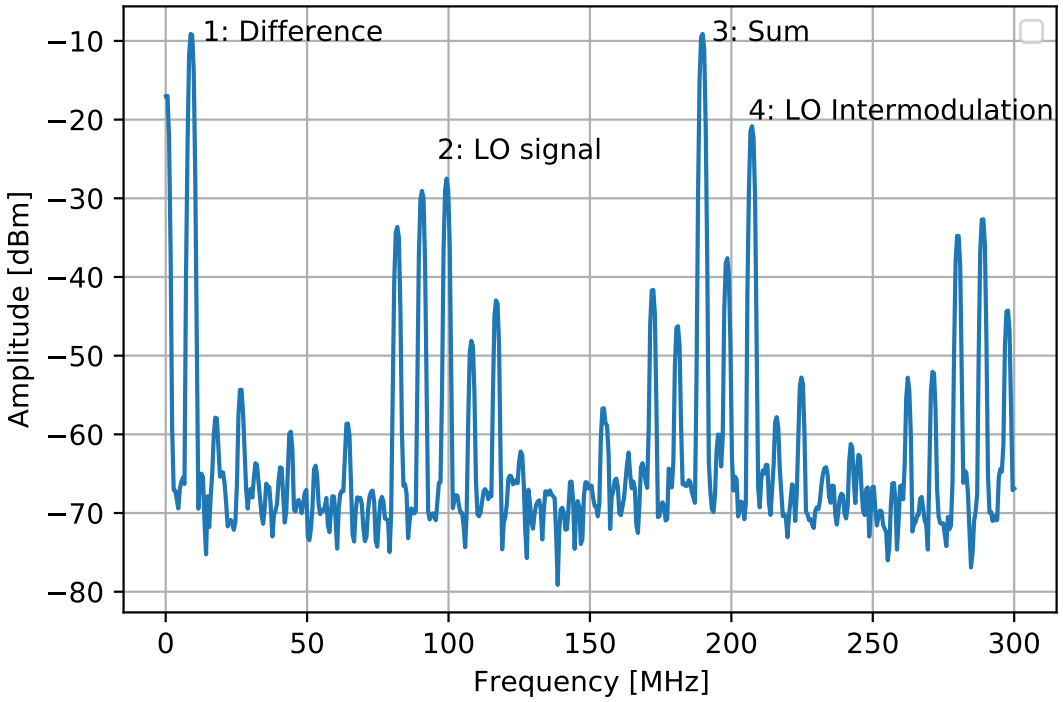

Figure 10: The output of a ring modulator mixer on a spectrum analyser. The LO signal is at 99MHz with 8dBm. The RF signal is at 90.6MHz with −2dBm. The frequencies with the highest amplitude are the sum frequency (peak 3) and difference frequency (peak 1). Their amplitude is equal and at −9dBm. Several intermodulation terms occur in the region of the sum and in the region of the original LO and RF frequencies, the most dominant $3LO - RF$ (peak 4) and the orignial LO frequency (peak 2)

99MHz and 8dBm. I adjust the RF frequency from 70MHz to 120MHz and I attenuate the RF amplitude to −2dBm. The mixer used is a SBL-1+ from MiniCircuits [11].

Figure 10 shows the output of the mixer with a RF frequency of 90.6MHz on a spectrum analyser.

Various frequencies appear in the output. I expect the sum frequency at 99MHz + 90.6MHz= 189.6MHz – Indeed, one sees a peak with the highest amplitude at this frequency. Similarly, the difference frequency occurs at $99 - 90.6 = 8.4$MHz. The power of both frequencies is at −9dBm.

The figure also shows a lot of intermodulation terms. The most dominant term, with an amplitude of −20dBm, occurs at 207MHz and is the fourth-order intermodulation term of the LO signal

$$3LO - RF = 3 \cdot 99 - 90 = 207\text{MHz}. \tag{13}$$

The input frequencies at 90MHz and 99MHz occur as well but they are damped to −28dBm. The next section examines the intermodulation terms in detail.

In the following, I demonstrate the behaviour of the mixer by tuning the RF frequency. The goal of the experiment is to show that the occurring frequencies are the sum frequency and the difference frequency, i.e., the goal is to show that the mixer behaves as expected. Figure 11 shows

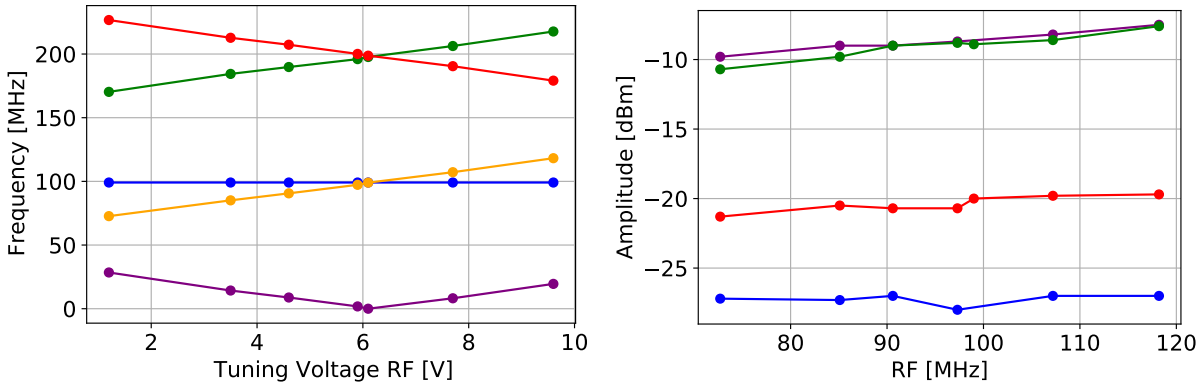

(a) Visible Frequencies

(b) Amplitudes

Figure 11: The most dominant on a spectrum analyser occurring output frequencies for a tuned RF input frequency at −2dBm. The LO signal is constant at 99MHz and 8dBm. Visible are the sum frequency (green line), the difference frequency (purple line), the fourth order LO intermodulation frequency (red line) and the input frequencies LO (blue line) and RF (orange line). The change in frequency confirms that the most dominant outputs are indeed the sum (constantly increasing) and the difference (minimum at similar input frequencies) as well as the intermodulation term, which corresponds to the sum frequency at approximately 6V (equal input frequencies) and decreases mirrored by the increase of the RF frequency. The amplitude of the signals stays constant for all RF values. The amplitude of the sum (green) and difference (purple) frequeny is equal and 10dB higher than the intermodulation signal (red). The amplitude of the LO signal (blue) is suppressed.

the change of the sum (green line), the difference (purple line), the dominant intermodulation term (red line) and the input frequencies RF (orange line) and LO (blue line). Figure 11a shows the change of the frequency with the RF tuning voltage, Figure 11b shows the change of the amplitudes with the RF frequency.

The change in frequency confirms that the most dominant outputs are the sum and the difference: The sum frequency, shown in green, increases constantly. The difference frequency, shown in purple, has its minimum at 0MHz for similar input frequencies. The LO signal is constant at 99MHz. The change of the RF signal corresponds to the VCO characteristic in Figure 8. Figure 11a also shows that the intermodulation term at approximately 6V corresponds to the sum of the corresponding frequencies. Further, its decrease is mirrored by the increase of the RF frequency. This observations shows that Equation 13 correctly predicts the observed sum frequency, difference frequency, and intermodulation term.

The change in amplitude is the same for all RF values. The amplitude of the intermodulation term (red) is constant and 10dB lower than the one of the sum signal. The amplitude of the LO signal (blue) is suppressed – however the intermodulation signal is only ten times lower than the sum and thus still relevant.

These results demonstrate that the mixer works as expected and generates the sum frequency and the difference frequency together with various intermodulation terms. The following section studies them in more detail.

4.3 Intermodulation Terms

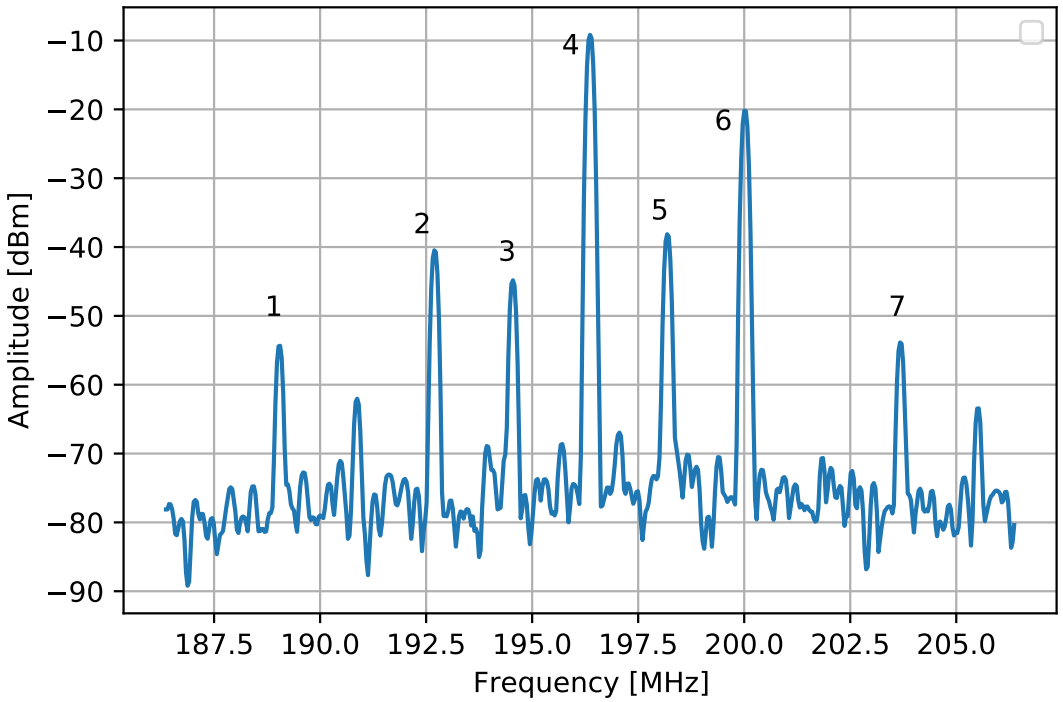

Figure 12: The output of a ring modulator at a spectrum analyser in the region of the frequency sum. The input signals are 99MHz as LO signal with $8dBm$ and 97.3MHz with −2dBm as RF signal. The occurring peaks are the sum frequency at 196MHz (peak 4), the fourth order intermodulation terms $3LO - RF$ at 200MHz (peak 6) and $3RF - LO$ at 193MHz (peak 2) and the double input frequencies $2LO$ at 198MHz (peak 5) and $2RF$ at 194.6MHz (peak 3). Higher-order intermodulation terms occur at $5LO - 3RF$ (peak 7) and $5RF - 3LO$ (peak 1).

As already discussed in the previous section, various intermodulation terms occur in the output of the mixer. The most dominant is the $3LO - RF$ fourth order intermodulation term. In this section, I allocate the other occurring terms.

Figure 12 shows the mixer output in the region around the frequency sum. I set the RF frequency to 97.3 MHz. The sum occurs at $99 + 97.3 = 196.3$MHz (peak 4). The fourth-order intermodulation terms are at $3LO - RF = 199.7$MHz (peak 6) and $3RF - LO = 192.9$MHz (peak 2). Their difference in amplitude is notable: The $3LO - RF$ power is at −20dBm, ten dBm less than the sum amplitude. The $3RF - LO$ term is at −40dBm and thus negligible. Higher-order terms at $2LO = 198$MHz (peak 5) and $2RF = 194.6$MHz (peak 3) occur as well. They do not differ noteworthy in amplitude: $2LO$ is slightly higher with −39dBm, but the difference to $2RF$ with −44dBm is small and in the same magnitude as the $3RF - LO$ term. The difference to the sum amplitude is 30dBm, which means that the amplitude is one-thousandth of the sum amplitude. Eighth-order intermodulation terms occur at $5LO - 3RF = 203$MHz (peak 7) and $5RF - 3LO = 189$MHz (peak 1), but their amplitudes are with less then −50dBm low. In-between peak 6 and peak 7 resp. peak 1 and peak 2 should be a peak at $4LO - 2RF = 201.4$MHz

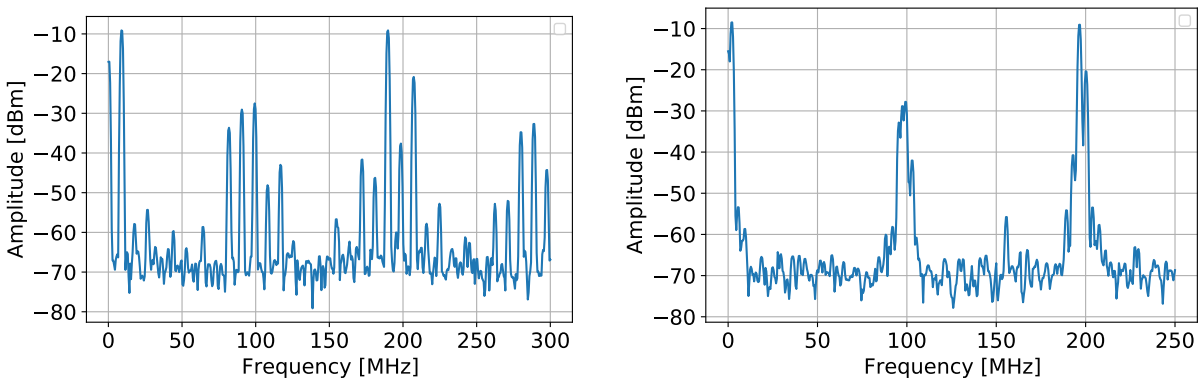

(a) RF at 90.6MHz

(b) RF at 97.3MHz

Figure 13: Comparison of the output of a mixer for two different RF frequencies, 90.6MHz and 97.3MHz, with an amplitude of −2dBm. The LO input signal is at 99MHz with 8dBm. In the first case, the intermodulation terms are clearly distinguishable. In the second case, the input frequencies are closer together and so are the intermodulation terms. They accumulate in the sum frequency region at 200MHz and in the region of the input frequencies at 100MHz.

resp. $4RF - 2LO = 191\text{MHz}$, but both are not significantly visible.

These observations confirm the theoretical description by Belevitch [3]. Visible terms are $mLO \pm nRF$ with m, n odd numbers.

To show the behaviour of the intermodulation terms, Figure 13 compares the mixer outputs for RF= 90.6MHz and RF= 97.3MHz. The different terms are clearly distinguishable in the first case. In the second case LO and RF are close together and so are the intermodulation terms. Two accumulations are visible: One in the sum frequency region at 200MHz and one at the region of the input frequencies at 100MHz.

4.4 Amplitudes of Input and Output Signals

Up to this point, I investigated the output of a mixer for different RF frequencies, but constant input levels: I set the RF level to −2dBm and the LO level to 8dBm. In this subsection, I test different RF and LO levels but hold their frequencies constant. I investigate the amplitudes of the output signals, consisting of the sum, the $3LO - RF$ and the $3RF - LO$ intermodulation term, depending on different input amplitudes. I focus on the sum since one has already seen in the previous subsection that the amplitudes of the difference frequency and sum frequency are at the same level.

First, I demonstrate the symmetric behaviour of a ring modulator by two measurements. The input signals are at $LO = 7.4\text{dBm}$ and $RF = -3.9\text{dBm}$. In the second measurement, I interchange the LO signal with the RF signal. In both cases, the sum amplitude is at −12dBm and the intermodulation terms are at $I_1 = -35\text{dBm}$ and $I_2 = -20\text{dBm}$, with I_2 related to the higher signal. That demonstrates that the circuit is completely symmetric. The local oscillator is always the signal higher in amplitude.

Figure 14 shows the amplitude difference between the LO signal and the sum signal (blue line) and the amplitude difference between the RF signal and the sum signal (orange line), depending

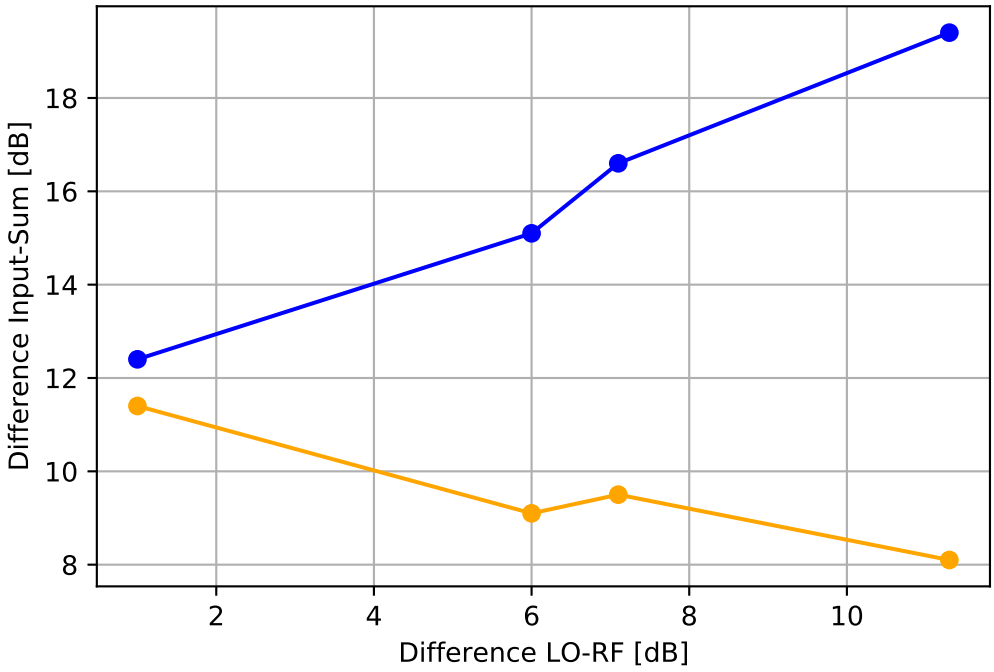

Figure 14: The difference in amplitude between the sum and the RF signal, shown in orange, respectively the sum and the LO signal, shown in blue, corresponding to different forced LO-RF differences. The LO values are 8.4dBm, 8.4dBm, 3.2dBm and 7.4dBm. The RF values are 7.4dBm, 2.4dBm, −3.9dBm and −3.9dBm. The orange line decreases and the blue line increases. The orange line corresponds with the *conversion loss* of a mixer: The difference between the RF signal and the sum signal. It is smaller the higher the LO-RF difference.

on the amplitude difference between LO and RF. The LO values are 8.4dBm, 8.4dBm, 3.2dBm and 7.4dBm. The RF values are 7.4dBm, 2.4dBm, −3.9dBm and −3.9dBm. The orange line decreases with an increasing difference, the blue line increases. That demonstrates that the amplitude of a mixer output is a fixed value smaller than the RF signal, which depends on the difference between RF and LO. The value is called conversion loss and corresponds with the orange line. The datasheet for the SBL-1+ mixer states that a conversion loss up 6dB is possible [11]. The LO level has to be at least at 7dBm, with the RF level at least 10dB smaller.

Figure 15 shows the amplitude difference between the sum signal and the $3LO - RF$ signal (red line) and the amplitude difference between the sum signal and the $3RF - LO$ signal (purple line), depending on the amplitude difference between LO and RF. The red line is nearly constant, meaning that the $3LO - RF$ intermodulation term is always around 10dB smaller in amplitude than the sum signal. The purple line increases with the LO-RF difference. Close to equal input amplitudes, both the red and the purple line are close together. The $3RF - LO$ term is thus not negligible in this region.

To summarise, a high LO level, i.e., at least 7dBm for the SBL-1+ ring modulator, and a low RF level, i.e., at least 10dB smaller than the LO level, are an ideal mixer configuration, leading to minimal conversion loss and a low $3RF - LO$ intermodulation term. That corresponds with

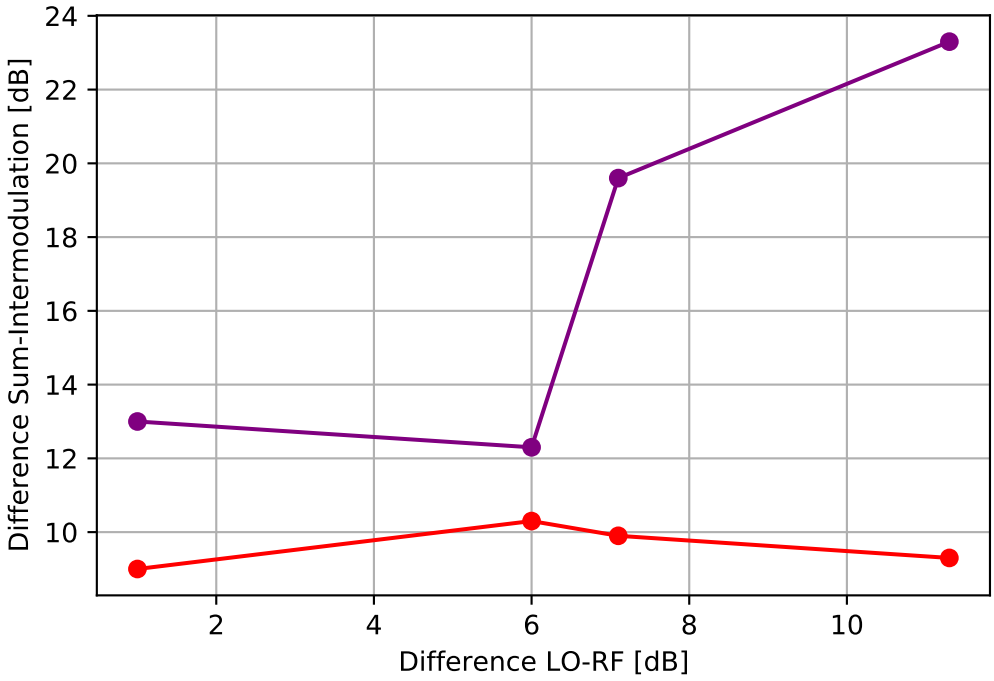

Figure 15: The difference in amplitude between the sum and the $3RF - LO$ intermodulation signal, shown in purple, respectively the sum and the $3LO - RF$ intermodulation signal, shown in red, corresponding to different forced LO-RF differences. The red line is nearly constant, meaning that the $3LO - RF$ intermodulation term is always around 10dB smaller in amplitude than the sum signal. The purple line increases with the LO-RF difference. Close to equal input amplitudes, both the red line and the purple line are close together. The $3RF - LO$ term is thus not negligible in this region.

the assumptions taken in section 3: A high LO level is needed to switch the diodes. A RF level in the same region leads to diode-switching as well. Thus, the RF level needs to be at least 10dB smaller.

5 Frequency Stabilisation by a Phase-Locked Loop

In this section, I explain an implementation to stabilise the frequencies based on a phase-locked loop (PLL). The circuit consists of two VCOs creating radio frequency signals to drive AOMs. Part of each signal is split off and used to lock the sum of the two frequencies on a third reference frequency, giving the Raman condition. The lock is done with a PLL, consisting of a phase-frequency detector (PFD) followed by a loop filter, which works as PI controller. The PFD compares both the sum and a reference frequency and generates two error signals proportional to the phase difference of the input signals.

First, I explain the theory of the PI controller used. Then I further discuss the circuit design and the performance of the implementation.

5.1 Theoretical Description of a PI Controller

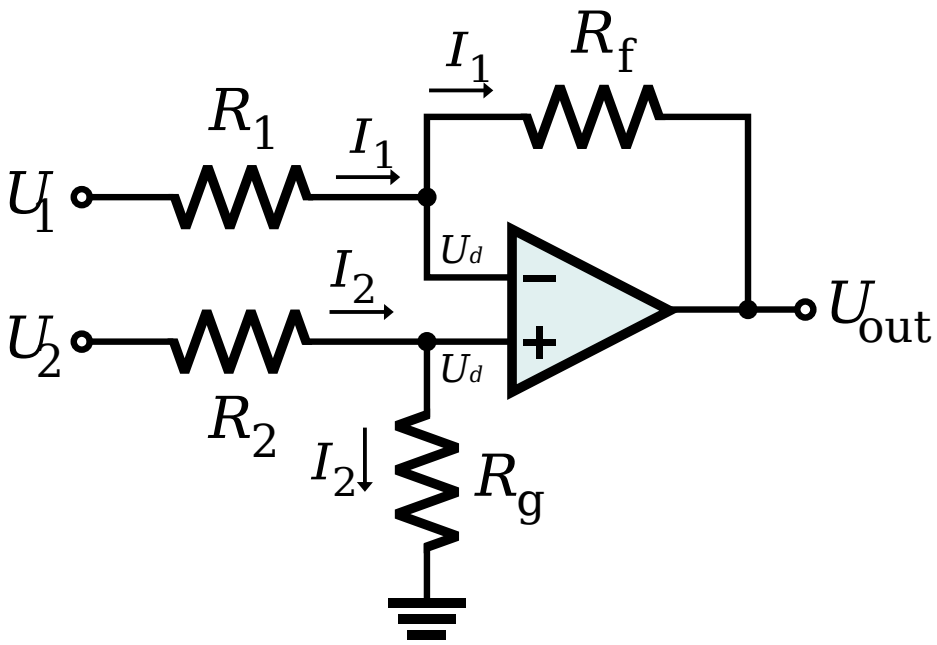

Figure 16: An Op-Amp Differential Amplifier. The output signal is proportional to the amplitude difference of signal U_1 and U_2. It can be used as a proportional controller in a feedback-loop. Adapted from [15]

To lock the frequency, a PI controller is needed which is given by the Loop filter. It compares the two input error signals, coming from the PFD, and generates an output signal to tune the second VCO, such that the input error signals are equal. The circuit resembles to an Op-amp differential amplifier (Figure 16) with additional capacitors at R_f and R_g.

To determine the gain of the loop filter, one has to do some calculations: The operational amplifier has a input resistance close to infinity, thus, the current I_2 through R_2 has to be equal to the current through R_g and similarly the current I_1 through R_1 equals the current through R_f. This leads to equations for the voltage U_d in front of the amplifier. The voltage difference of the two inputs is pulled to zero by the op-amp, thus the voltage U_d is the same for both

inputs.

$$U_d = I_2 R_g \tag{14}$$

$$U_2 = \frac{R_2 + R_g}{I_2} \tag{15}$$

$$\rightarrow U_d = \frac{U_2 R_g}{R_2 + R_g} \tag{16}$$

And similarly, using Kirchhoff's law:

$$I_1 = \frac{U_1 - U_d}{R_1} = \frac{U_d - U_{out}}{R_f} \tag{17}$$

$$\rightarrow U_{out} = R_f (U_d \frac{R_1 + R_f}{R_1 R_f} - \frac{U_1}{R_1}) \tag{18}$$

Putting both formulas together, one gets

$$U_{out} = U_2 \frac{R_g}{R_1} \frac{R_1 + R_f}{R_2 + R_g} - U_1 \frac{R_f}{R_1}. \tag{19}$$

Setting $R_1 = R_2$ and $R_f = R_g$, the equation simplifies to

$$U_{out} = \frac{R_f}{R_1}(U_2 - U_1) \tag{20}$$

and one can directly see that the output signal is proportional to the difference of the input amplitudes with a gain of $G = \frac{R_f}{R_1}$. This is a proportional controller.

With just a proportional controller, one can never reach an error of zero, since it requires an error to generate the proportional response. To get rid of this problem, one combines the proportional controller with an integral term. To get this integral term, one uses capacitors at R_f and R_g.

They can be interpreted as an AC resistor with an impedance of $R = \frac{1}{i\omega C}$ with $\omega = 2\pi f$. This leads to a series connection of resistors and R_f changes to

$$R_f = \tilde{R}_2 + \frac{1}{i\omega C} \tag{21}$$

with $\tilde{R}_2$ as resistor and C as capacitor. Finally, one gets

$$U_{out} = (\underbrace{\frac{\tilde{R}_2}{R_1}}_{P} + \underbrace{\frac{1}{i\omega C R_1}}_{I})(U_2 - U_1) \tag{22}$$

with a proportional control term P and an integral control term I.

The integral term increases the output signal to the error and the duration of a specific error signal. The output signal is higher the longer an error occurs.

The characteristic of the PI controller is depicted in Figure 17. The specific values are: $R_1 = 200\Omega$, $\tilde{R}_2 = 100\Omega$ and $C = 100\text{nF}$. These values are used for the final design of the PLL. U_1 and U_2 are generated by the PFD and are in our case between $3V$ and $5V$, thus

$U_1 = 3V$, $U_2 = 5V$ in the graph. The blue line is the characteristic of the full PI controller. The orange line is the characteristic of only the integral term, the green line the characteristic of the proportional term. The interception point is at $f = \frac{1}{2\pi C\tilde{R}_2}$.

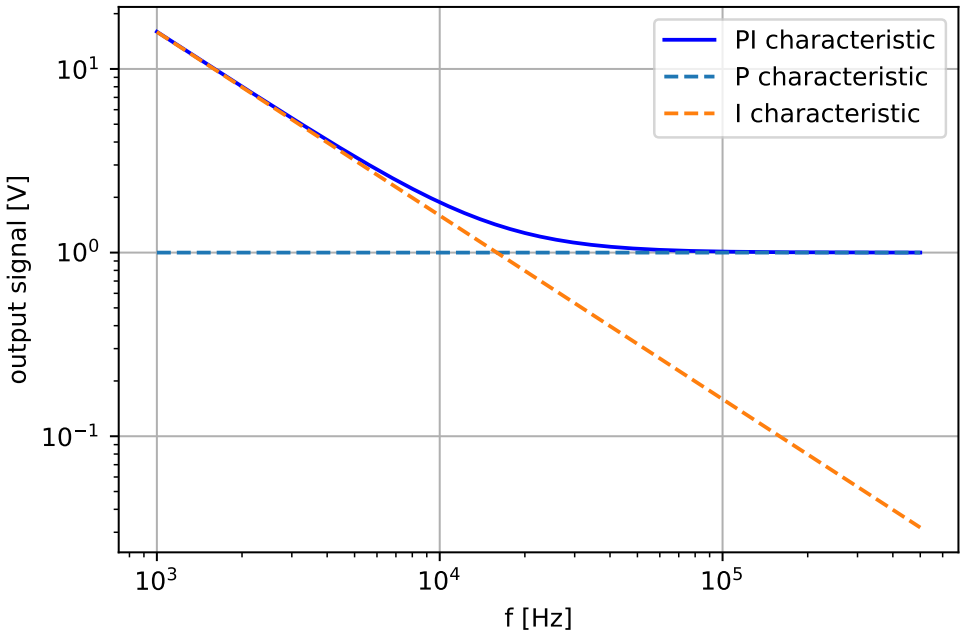

Figure 17: The calculated characteristics of the PI controller used. The specific values are: $\tilde{R}_1 = 200\Omega$, $\tilde{R}_2 = 100\Omega$, $C = 100\text{nF}$, $NU = 3V$, $ND = 5V$. The orange line is the characteristic of the integral term, the green line the characteristic of the proportional term. The blue line is the combined characteristic of the PI controller. The interception point is at $f = \frac{1}{2\pi C\tilde{R}_2}$.

5.2 Circuit Design

Here, I explain the implementation of the phase-locked loop and how it can be used to generate the two frequencies. Figure 18 shows the implemented circuit. Two VCOs generate the frequencies to drive AOMs. To control their frequency, a directional coupler splits the VCO power. One VCO generates the local oscillator signal: 90% goes to the mixer and 10% to an AOM. The other VCO generates the RF signal with only 10% going to the mixer and 90% going to the other AOM.

The mixer output is the sum and the difference of the two input frequencies and several intermodulation terms. Only the sum is of interest: a high pass filter suppresses the difference signal.

The phase-frequency detector compares the sum with the Raman condition reference signal at 230.85MHz and generates two voltage signals depending on the phase difference between input signals. The phase-frequency detector used is *HMC3716LP4E* from Analog Devices. It is a digital phase frequency detector and optimised for high frequencies from 10 to 1300MHz. The output for a forced frequency difference of 11Hz is depicted in Figure 20: The two error

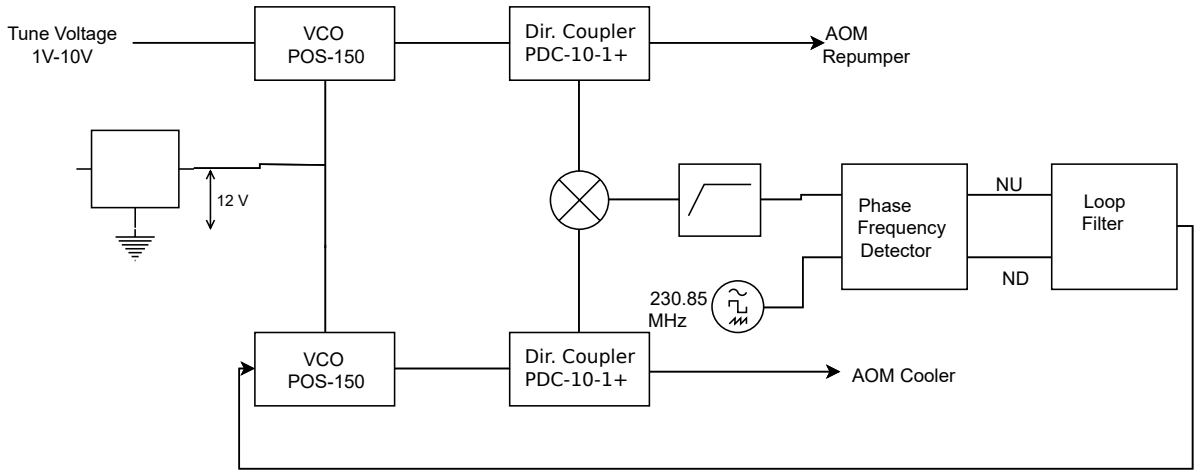

Figure 18: Circuit to stabilise frequencies using a phase-locked loop. Two VCOs drives the AOMs. Their supply voltage is $12V$. The tuning voltage is adjustable and proportional to the outcoming frequency. One VCO is manually tuned, the other one is controlled by a phase-locked loop such that their frequency sum, generated by a mixer, is locked to a reference signal. The phase-locked loop consists of a phase-frequency detector, which generates two error signals proportional to the phase difference of the input signals, and a loop filter, working as a PI Controller.

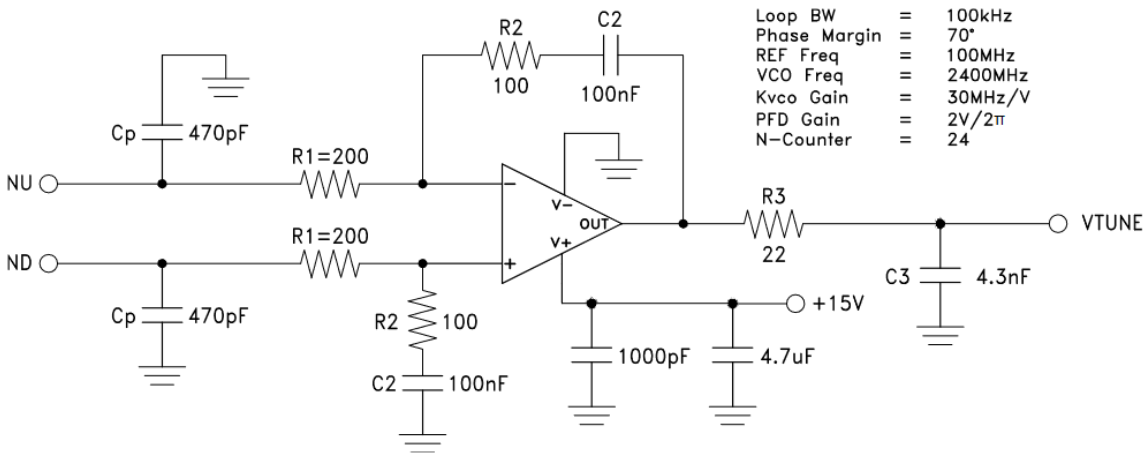

Figure 19: A typical loop filter to integrate the NU and ND pulses from the phase frequency detector. It works as a PI Controller: The output signal VTUNE is proportional to the voltage difference of NU and ND and their integrated amplitude difference and is used to drive a VCO. Taken from [1]

signals, NU and ND, are between 3V and 5V. ND is constant as long as one input is higher in frequency. By forcing the frequency difference the other way round, NU would be constant. Both signals are the same when the phase difference is zero for all times. LD is the lock detect signal: It is constant at $5V$ as soon as the phase difference is zero and serves as a monitoring signal [5, 1].

The Loop filter works as a PI controller, as explained in subsection 5.1, and generates the tuning voltage for the second VCO. It compares the two input error signals and controls the tuning voltage such that their voltage difference is zero. This is reached when NU equals ND. In

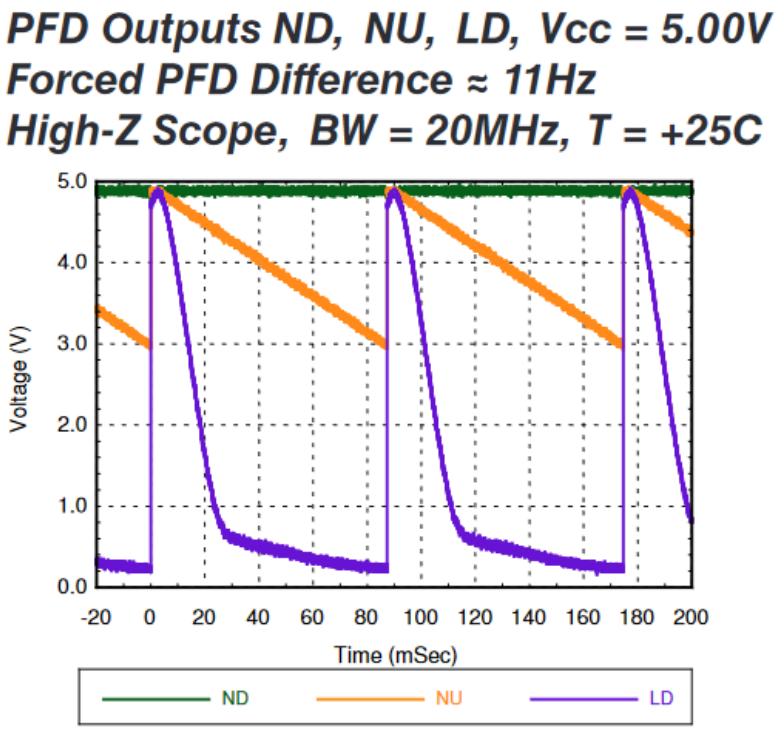

Figure 20: Error signals NU and ND of the Phase Frequency Detector HMC3716LP4E at a forced input frequency difference of 11Hz. LD is the lock detect signal and serves as monitoring signal. It is constant at 5V as soon as the phase is locked. Taken from [1].

Figure 19, one can see the circuit with the values used for resistors and capacitors. The 470pF capacitors (C_p) at the beginning are decoupling capacitors to filter noise at higher frequencies.

I implemented the circuit on a copper plate with components from Mini-Circuits and included the PFD and the loop filter with SMA connectors. The loop filter is a modified *THS4031* high-speed operational amplifier evaluation module by Texas Instruments [14]. Furthermore, I implemented the loop filter ciruit on a breadboard to test its PI performance with different resistor values. The process variable is the intensity of a bulk lamp, measured by a photodiode. The PI controller generates its tuning voltage. The reference signal is given by a frequency generator.

5.3 Performance

In this subsection, I show the performance of the PI controller and the PLL and conclude with the experimental behaviour of the above explained circuit.

First, I tested the PI controller, using frequencies low enough to use a standard operational amplifier and potentiometers. This has the advantage of making the resistors scaleable to test different gains of the PI controller. I successfully locked the intensity of a bulk lamp with the default values given in Figure 19.

I tested the PLL in a simplified version of Figure 18, changing the input of the PFD to simply one VCO, without mixer, and one reference signal. The Output of the loop filter tunes

the VCO. I stabilised VCO frequencies in the range of 80 to 250 MHz.

Finally, I tested the full circuit shown in Figure 18. I tested the first VCO in the range of 90 to 140MHz and set the reference signal to 230.85MHz. For frequencies smaller than 105MHz and greater than 125MHz, the PLL successfully locked the sum. In the range of equal frequencies ($f = 115$MHz), locking was not possible.

An explanation for this behaviour is that the mixer intermodulation terms disturb the PFD and thus the lock. In the range of equal input frequencies, the mixer intermodulation terms are close to the sum frequency. This is depicted in Figure 13b.

Since for grey molasses, we need stable locks in the range of 100 to 130MHz, and especially at equal input frequencies, this implementation can not be used here.

In the next section, I present another solution.

6 Frequency Stabilisation by Subtracting Frequencies

In this section, I introduce another method to stabilise the Raman condition, based only on a mixer and one VCO: One VCO signal is splitted, a part is going to one AOM, the other part is mixed with the reference signal. The difference of both signals is used to drive the other AOM. I conclude with the installation in the experimental setup of the grey molasses and their performance.

6.1 Circuit Design

First, I explain the circuit of this implementation, shown in Figure 21.

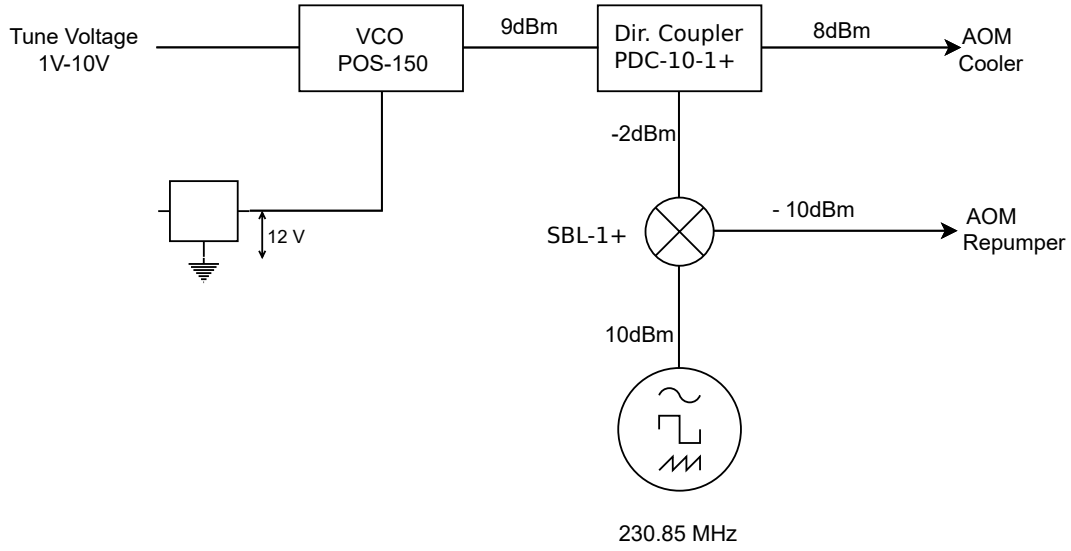

Figure 21: Circuit to stabilise the sum of two frequencies. One frequency is generated by a VCO. The power is split, one part drives the Cooler AOM, the other part is mixed with a reference signal at the raman condition. The difference of both signals drives the Repumper AOM.

The VCO is tuned by a computer channel to get an output frequency in the range of 100 to 130MHz. The signal is split with a directional coupler. 10 percent of the signal goes to the mixer. The other 90 percent drives the Cooler AOM.

The other mixer input is the reference signal at 230.85MHz. Since we use double pass AOMs, it is half of the raman frequency. In this implementation, it is given by a frequency generator. The power can be easily regulated. It is set to 10dBm to serve as local oscillator.

The mixer output is the sum and the difference of both signals. Now, we use the difference signal: it gives the other frequency, used to drive the Repumper AOM:

$$230.85\text{MHz} - f_{\text{Cooler}} = f_{\text{Repumper}}. \tag{23}$$

By rearranging the formula,

$$f_{\text{Cooler}} + f_{\text{Repumper}} = 230.85\text{MHz}, \tag{24}$$

it can be easily seen that this is a sufficient approach.

One does not need a low pass filter after the mixer since the AOM has a band pass behaviour, filtering out the sum frequency.

I installed the circuit into the experiment using new AOM boards. Analogue computer channels control the frequency of the Cooler and furthermore the power of both the Cooler and Repumper. A frequency generator sets the Raman condition. A computer program controls the molasses and sets the hold time and the ramping time as well as the start and the end frequency of the Cooler.

6.2 Performance

In this subsection, I talk about the performance of the molasses using the above explained circuit. I explain how different parameters affect the performance and I compare the final temperature with the one of the old molasses.

As explained in section 2, the relevant parameters are the Raman condition, the hold time, the ramping time and the start and the end frequency of the Cooler. The start frequency defines the detuning at the beginning. The end frequency defines the detuning after ramping. The Repumper follows the Cooler in this setup and is thus not individually adjustable.

The performance of the molasses is given by the phase space density after ramping. A high phase space density is reached for a high atom number and low temperature of the atoms. The latter can be estimated by the width after a fixed time of flight ($15ms$ here).

In the following, the atom number is given in arbitrary units and the width σ_x is given in pixels.

Raman condition

First, I scan the Raman condition. The theoretical value is at 230.85MHz. In Figure 22 one can see the atom number and the width of the atomic cloud, σ_x, at the corresponding value for the Raman condition. The orange points are scans from 228.85MHz to 231.85MHz and the blue points are finer scans with smaller stepsize. They are going from 230.5MHz to 231.2MHz. One can clearly see that a change in the Raman condition affects the atomic cloud after the molasses. In Figure 22a one can see that the atom number is at a plateau between 230.6MHz and 231.0MHz. The width, as seen in Figure 22b, has a minimum at 230.95MHz. This is close to the theoretical value.

Start frequency Cooler

Here, I sweep the start frequency of the Cooler. The expected value is near to resonance at $\frac{230.85}{2}$MHz = 115.4MHz, since detuning has to be small, but still blue-detuned to get a maximum cooling force.

Figure 23 shows the atom number and the distribution width for start cooler frequency tuning voltages from $6V$ to $10V$. This corresponds to 100MHz and 125MHz. In Figure 23a, one can see how the atom number changes with frequency, and in Figure 23b one can see how the width of the atom cloud changes. The atom number has its maximum with 52000 atoms at 8.4V. 8.4V

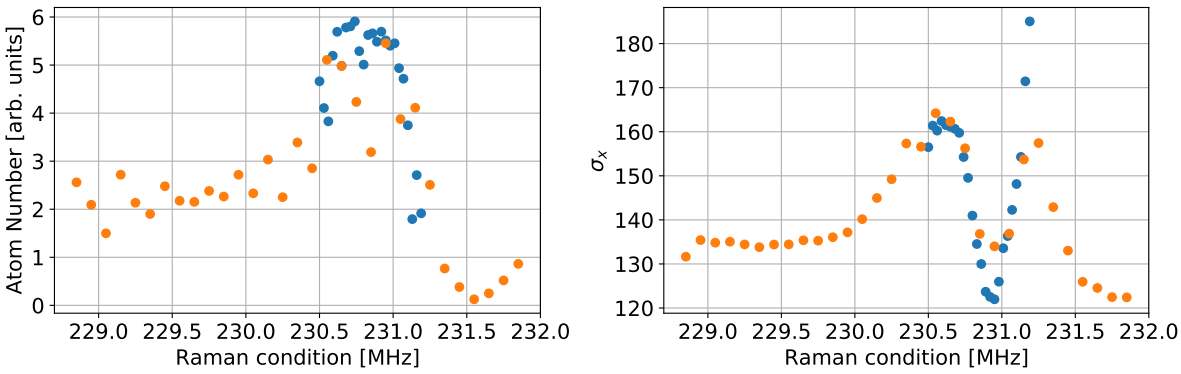

(a) atom number (b) σ_x

Figure 22: The atom number and distribution width after $15ms$ time of flight for different Raman condition frequencies. A minimum in the distribution width appears at 230.95MHz with high atom number, which corresponds to a high phase-space density close to the theoretical value at 230.85MHz.

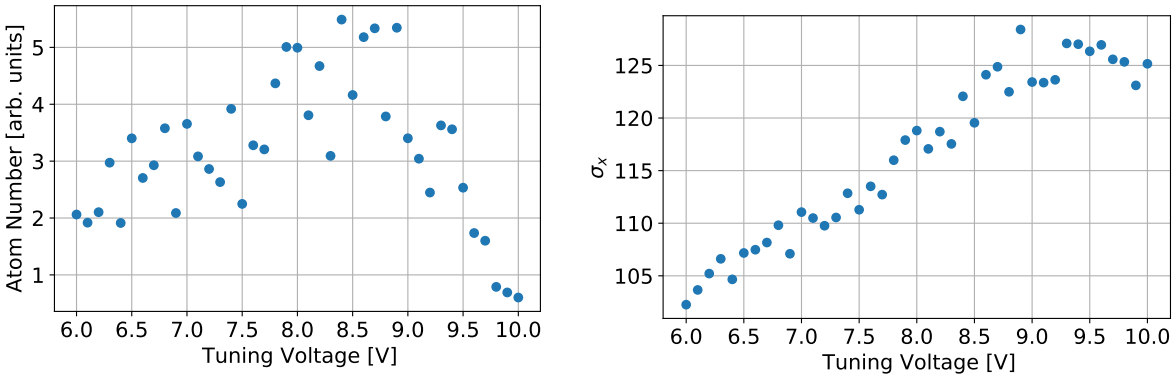

(a) atom number (b) σ_x

Figure 23: The atom number and distribution width after $15ms$ time of flight for the start frequency of the Cooler, tuned from 6V (100MHz) to 10V (125MHz). A high atom number and corresponding low width is given at 8.5V which corresponds with 115MHz to the theoretical expectation (close to resonance).

corresponds to 114.9MHz, which matchs the expected value. The distribution width is linearly increasing.

End frequency Cooler

Next, I sweep the end frequency of the Cooler. It defines the maximum detuning to which the molasses ramp and thus, should be lower than the frequency at resonance. Figure 24 shows the atom number and the width for end cooler frequencies from 4.5V (92MHz) to 8.5V (115MHz). A good frequency value is at 6.4V with 103.2MHz: The atom number is high, and σ_x is low. The atom number increases up to that value and saturates. The width increases the whole time.

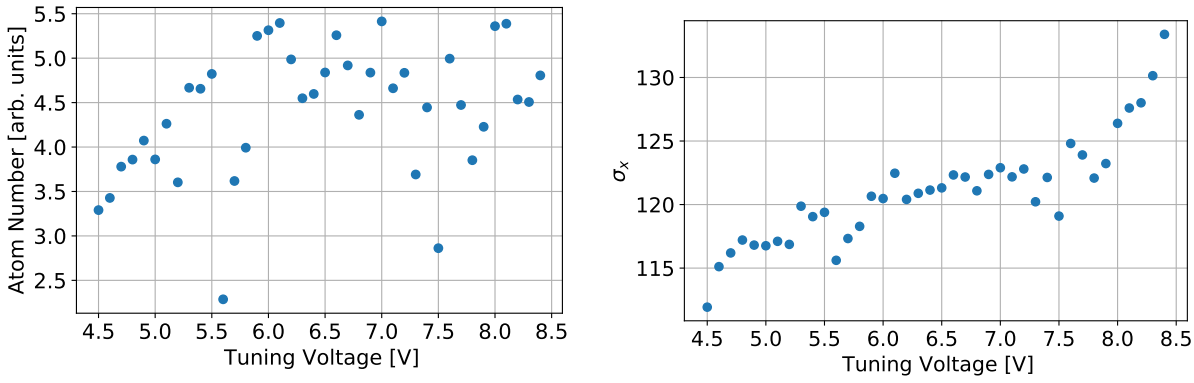

(a) atom number (b) σ_x

Figure 24: The atom number and distribution width after $15ms$ time of flight for the end frequency of the Cooler, tuned from from 4.5V (92MHz) to 8.5V (115MHz). 6.4V (103.2MHz) is a good value for the end frequency: The atom number increases up to that value and saturates. The width increases the whole time.

Hold time

The hold time defines the waiting time at the beginning where the frequency of the cooler is held constant near resonance and defines the time the atoms need to slow down. Salomon et al. [13] found this time to be less than $2ms$.

In Figure 25 one can see the performance for different hold times: Both the atom number and the width increases in the first $1.5ms$. This is the time needed to cool down and a good value to proceed with. Additionally, it is close to the value found by Salomon et al.. After that, both the atom number and the width saturate.

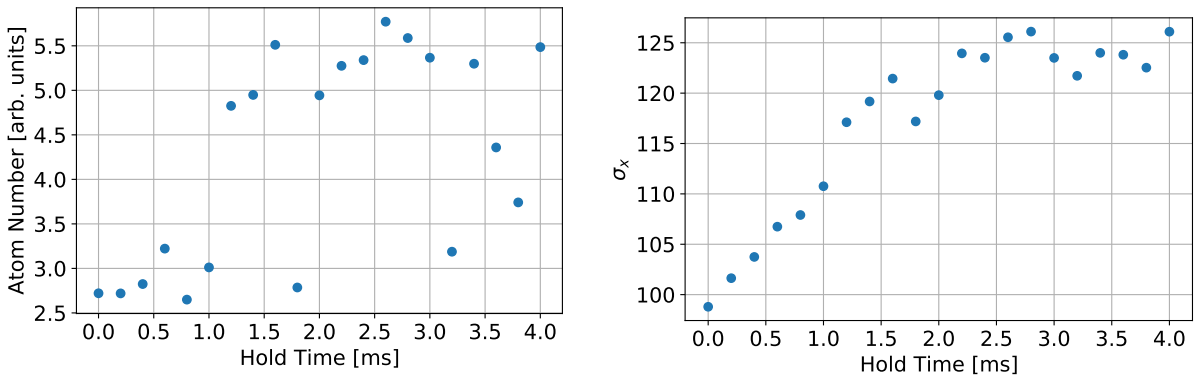

(a) atom number (b) σ_x

Figure 25: The atom number and distribution width σ_x after $15ms$ time of flight for different hold times up to $4ms$. The atom number and distribution width increases the first $1.5ms$. After that, both the atom number and the width saturate. $1.5ms$ is thus the time the molasses need to cool the atoms down and a good value to proceed with.

Ramping time

Finally, I investigate different ramping times. The ramping time is the time needed to linearly sweep from the start frequency to the end frequency, i.e., increasing detuning, after holding the molasses constant near resonance.

In Figure 26 the ramping time is tuned from $0.5ms$ to $5ms$. A good value with high atom number and small σ_x is $2.3ms$.

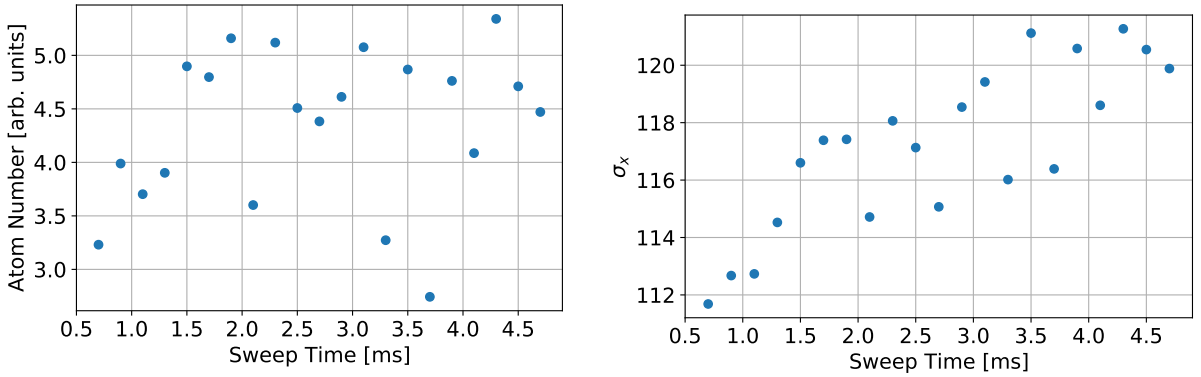

(a) atom number

(b) σ_x

Figure 26: The atom number and distribution width σ_x after $15ms$ time of flight for different ramping times, up to $5ms$. The ramping time defines how fast the molasses increase the detuning. A good value with high atom number and low σ_x is $2.3ms$.

Comparison to performance of the old setup

The performance of the grey molasses is given by the mean atom number and the temperature. One can determine the temperature as explained above. Different parameter settings determine the temperature. With the new molasses, I got temperatures up to $7\mu K$. With the final parameters, the temperature is at $8\mu K$, but the atom number is higher.

The mean atom number is determined by averaging over 20 shots for the old molasses and 73 shots for the new molasses.

The mean atom number in arbitrary units of the new molasses is

$$4.84 \pm 0.61. \tag{25}$$

The temperature of the old molasses is $11\mu K$. The mean atom number is

$$4.01 \pm 0.62. \tag{26}$$

Thus, the new molasses are an improvement. The final temperature is with $8\mu K$ 30% lower than the temperature after the old molasses. The mean atom number is 20% higher with unchanged standard derivation.

Furthermore, the new molasses worked stable for at least three months and thus demonstrated long-term stability.

7 Conclusion and Outlook

In this thesis, I designed, implemented and tested a new setup to generate the frequencies for grey molasses cooling.

First, I explained a ring modulator output and showed that higher order mixing terms play an important role. I investigated the amplitude fractions of the several occurring mixing terms. Dominant is the fourth order mixing term with three times the local oscillator frequency minus the RF frequency. Furthermore, I investigated the correct usage of a mixer. It is beneficial to have a local oscillator power higher than the level given in the mixer data sheet. The RF signal power should be at least 10dBm smaller to suppress other intermodulation terms. The level of the mixer output depends only on the RF power.

Second, I introduced a first method to fix the Raman condition, based on a phase locked loop. I showed that the phase-locked loop works well, but cannot be used for grey molasses cooling. The lock does not work near to resonance, however, this is an important requirement. I explained why the lock does not work near resonance by investigating the working principle of a frequency mixer. Another case of application for the phase-locked loop is a laser beat lock, where the beat signal of two lasers is locked to a reference signal. In the BECK experiment, an example are the absorption imaging lasers at the D2 line.

Finally, I introduced a second method to produce the desired frequency by directly generating the difference of a stable reference frequency and an input frequency, which reduces degrees of freedom. After implementation and optimisation, the new molasses cool down to $8\mu K$ with a mean atom number of 4.84 ± 0.61 arb units. Furthermore, the setup demonstrated long-term stability. With other parameter settings, I showed that temperatures up to $7\mu K$ are possible. In comparison, the old molasses cooled down to $11\mu K$ with a mean atom number of 4.01 ± 0.62 arb units.

References

[1] Analog Devices. *HMC3716LP4E HBT Digital Phase Frequency Detector*. [Online; accessed June 10, 2021]. URL: https://www.analog.com/media/en/technical-documentation/data-sheets/HMC3716.pdf.

[2] A. Ashkin et al. "Observation of a single-beam gradient force optical trap for dielectric particles". In: *Optics letters* 11.5 (1986), pp. 288–290.

[3] V Belevitch. *Non-linear effects in ring modulators', Wireless Engineer, 26*. 1949.

[4] C. N. Cohen-Tannoudji and W. D. Phillips. "New mechanisms for laser cooling". In: *Phys. Today* 43.10 (1990), pp. 33–40.

[5] I. Collins. "Phase-Locked Loop (PLL) Fundamentals". In: *SSB* 130.140 (2018), p. 150.

[6] J. Dalibard and C. Cohen-Tannoudji. "Laser cooling below the Doppler limit by polarization gradients: simple theoretical models". In: *JOSA B* 6.11 (1989), pp. 2023–2045.

[7] M Hufschmid. *Zur Funktionsweise des Diodenringmischers*. [Online; accessed Mai 27, 2021]. URL: https://www.informationsuebertragung.ch/Extras/Mischer.pdf.

[8] M Landini et al. "Sub-Doppler laser cooling of potassium atoms". In: *Physical review A* 84.4 (2011), p. 043432.

[9] P. D. Lett et al. "Observation of Atoms Laser Cooled below the Doppler Limit". In: *Phys. Rev. Lett.* 61 (2 1988), pp. 169–172. DOI: 10.1103/PhysRevLett.61.169. URL: https://link.aps.org/doi/10.1103/PhysRevLett.61.169.

[10] D. McCarron. *A guide to acousto-optic modulators*. [Online; accessed June 19, 2021]. 2007. URL: http://massey.dur.ac.uk/resources/slcornish/AOMGuide.pdf.

[11] Mini-Circuits. *SBL-1+*. URL: https://www.minicircuits.com/pdfs/SBL-1+.pdf.

[12] W. D. Phillips and H. Metcalf. "Laser deceleration of an atomic beam". In: *Physical Review Letters* 48.9 (1982), p. 596.

[13] G. Salomon et al. "Gray-molasses cooling of 39K to a high phase-space density". In: *EPL (Europhysics Letters)* 104.6 (2014), p. 63002.

[14] Texas Instruments. *THS4031 High-Speed Operational Amplifier Evaluation Module User's Guide*. [Online; accessed June 19, 2021]. 1999. URL: https://www.ti.com/lit/ug/slou030/slou030.pdf?ts=1624098380980&ref_url=https\%253A\%252F\%252Fwww.ti.com\%252Ftool\%252FTHS4031EVM.

[15] Wikipedia, the free encyclopedia. *Op-Amp Differential Amplifier*. [Online; accessed June 10, 2021]. 2021. URL: https://upload.wikimedia.org/wikipedia/commons/a/a2/Op-Amp_Differential_Amplifier.svg.

[16] Wikipedia, the free encyclopedia. *Ring modulation example of Diode-clipping or 'chopper' RM*. [Online; accessed Mai 27, 2021]. 2021. URL: https://upload.wikimedia.org/wikipedia/commons/0/0d/Ring_modulation_two_forms_Diode-clipping_or_\%27chopper\%27_RM.svg.

Danksagung

An dieser Stelle möchte ich mich zuerst bei Herrn Prof. Markus K. Oberthaler für die Aufnahme in seine Arbeitsgruppe und das spannende Thema bedanken.

Außerdem möchte ich dem gesamten BECK-Team danken: Für die Hilfestellung bei der praktischen Umsetzung, für ausführliche physikalische Erklärungen und zu guter Letzt für das zahlreiche Korrekturlesen der Arbeit. Ich hatte immer das Gefühl, zu jeder Zeit mit meinen Fragen und Problemen zu euch kommen zu können, dankeschön dafür!

Erklärung

Ich versichere, dass ich diese Arbeit selbstständig verfasst und keine anderen als die angegebenen Quellen und Hilfsmittel benutzt habe.

Heidelberg, den 21.06.2021